From Ultraslow to Fast Lithium Diffusion in the 2D Ion Conductor $Li_{0.7}TiS_2$ Probed Directly by Stimulated-Echo NMR and Nuclear Magnetic Relaxation

M. Wilkening,* W. Küchler, and P. Heitjans†

Institute of Physical Chemistry, University of Hannover, Callinstr. 3-3a, D-30167 Hannover, Germany

(Received 15 January 2006; published 8 August 2006)

^{7}Li stimulated-echo NMR and classical relaxation NMR techniques are jointly used for the first time for a comprehensive investigation of Li diffusion in layer-structured $Li_{0.7}TiS_2$. One single 2D Li diffusion process was probed over a dynamic range of almost 10 orders of magnitude. So far, this is the largest dynamic range being measured by ^{7}Li NMR spectroscopy directly, i.e., without the help of a specific theoretical model. The jump rates obey a strict Arrhenius law, determined by an activation energy of 0.41(1) eV and a preexponential factor of $6.3(1) \times 10^{12}$ s^{-1}, and range between 1×10^{-1} s^{-1} and 7.8×10^8 s^{-1} (148–510 K). Ultraslow Li jumps in the kHz to sub-Hz range were measured directly by recording ^{7}Li spin-alignment correlation functions. The temperature and, in particular, the frequency dependence of the relaxation rates fully agree with results expected for 2D diffusion.

DOI: 10.1103/PhysRevLett.97.065901 PACS numbers: 66.30.−h, 76.60.Lz, 82.47.Aa

In the last decade the investigation of solid Li ion conductors has developed into a vast research topic with several hundreds of papers per year. The reason is that Li ion conductors serve both for applications in, e.g., batteries with high energy density and for fundamental studies of the lightest ion besides hydrogen concerning mechanisms, influence of dimensionality, or quantum effects in diffusion. Unfortunately, due to the lack of a suitable radioactive Li isotope, the standard tracer diffusion technique is not applicable. Alternatively, Li diffusion can be probed on different time scales by nuclear magnetic resonance (NMR) techniques [1]. This Letter emphasizes the direct, i.e., model-independent, measurement of ultraslow Li jumps in TiS_2 with rates from the kHz to the sub-Hz range by ^{7}Li spin-alignment echo (SAE) NMR. The method was originally developed for deuterons by Spiess [2] and, quite recently, successfully applied also to spin-3/2 nuclei, like ^{9}Be [3] and ^{7}Li [4]. Recording two-time ^{7}Li SAE single-particle correlation functions enables direct access to Li jump rates. The method is applicable at relatively low temperatures, so that it is expected to become one of the leading techniques for the study of Li dynamics in numerous, possibly heat-sensitive Li conductors. Compared to two-dimensional (2D) Li exchange NMR [5], which is also capable to measure very slow Li jumps directly in the present sense, ^{7}Li SAE NMR is much less time consuming and applicable to a much broader class of crystalline and even amorphous materials. Furthermore, a much larger dynamic range can be investigated which is about four decades in the present study. Two-dimensional NMR experiments can be carried out only if a direct Li exchange process becomes visible in the 2D spectra. To our knowledge, only few Li 2D NMR experiments have been performed until now; see, e.g., Refs. [5–7].

Here, polycrystalline layer-structured Li_xTiS_2 with $x = 0.7$ was chosen as a unique model substance for a comprehensive investigation of 2D Li diffusion. For the first time, jump rates from ^{7}Li SAE NMR with values down to the sub-Hz range were systematically compared to those obtained from classical ^{7}Li NMR relaxation probing Li diffusion on a much shorter time scale with jump rates up to the GHz range. Diffusion induced spin-lattice relaxation rates in the laboratory ($T_{1\mathrm{diff}}^{-1}$) and rotating frame ($T_{1\varrho\mathrm{diff}}^{-1}$) were measured. Jump rates from relaxation NMR were determined independently of a specific model solely from the frequency dependent positions (on the temperature scale) of the maxima of the corresponding relaxation rate peaks. The measurement of spin-spin relaxation rates (T_2^{-1}) complements the present study. By combining these four different NMR methods, one and the same Li diffusion process was detected and probed precisely over a dynamic range of about ten decades. To our knowledge, this is so far the largest range being measured by ^{7}Li NMR spectroscopy directly, i.e., without involving a theoretical model which correlates experimental data with microscopic diffusion parameters. While there have been several papers reporting jump rates over a large range, in particular, in the case of Li metal [8–10], these have been evaluated using not only the maxima but rather by fitting various models to the flanks of the relaxation peaks.

Layered TiS_2 is one of the best investigated materials for reversible, topotactical intercalation [11] with, e.g., Li^+ ions. The thermal stability of Li_xTiS_2 and its simple layered structure (CdI_2-type structure, space group $P\bar{3}m1$) make it a singularly well-defined fast Li conductor for the study of cation diffusion being confined to two dimensions, i.e., the plane (“van der Waals gap” [11]) between the TiS_2 layers. Single phase Li_xTiS_2 is stable in the entire intercalation range $1 \leq x < 0$. Li ions in layered TiS_2 reside preferentially in the octahedral (1b) rather than in the tetrahedral (2d) sites [12] between the TiS_2 layers. Temporary occupation of 2d sites between two octahedra has been suggested to serve as a transition structure for Li^+ hopping [13]. The sample was prepared via conventional

solid state synthesis. A mixture of titanium and sulfur powders in the ratio 1:2.1 was heated at 870 K for about two weeks in an evacuated quartz tube. Excess sulfur was removed at 420 K under vacuum. Li was intercalated at room temperature in inert gas atmosphere using n-butyl lithium. The sample was characterized by x-ray diffraction and ^{7}Li NMR spectroscopy [14].

In a SAE NMR experiment the spins are labeled by the interaction of the nucleus with an electric field gradient, produced by the distribution of electric charge carriers in the neighborhood of the nuclei. Spin-alignment echoes as a function of mixing time t_m and at constant evolution time t_p are sampled employing the Jeener-Broekaert radio frequency pulse sequence 90°_x-t_p-45°_y-t_m-45°-t [15]. Jumping of the ion between sites j and k with different quadrupole frequencies ω_{Q_j} and ω_{Q_k} causes a time dependence of $\omega_Q(t_m)$ and thus leads to an echo decay from an initial echo amplitude at $t_m = 0$ to a final state amplitude at $t_m \gg 0$. Here, octahedral and tetrahedral sites with quite different ω_Q ($\omega_Q/2\pi$ values being in the kHz range [14]) are involved in the diffusion process, as can be shown by evolution time dependent SAE NMR measurements [16] indicating the migration pathway: $1b \rightarrow 2d \rightarrow 1b'$. In Fig. 1 a typical decay of ^{7}Li SAE amplitudes $S_2(t_p, t_m, t)$ recorded for $t_p = 15\ \mu$s and $\omega_0/2\pi = 155$ MHz is shown for polycrystalline $Li_{0.7}TiS_2$. ω_0 is the angular Larmor frequency. NMR measurements were performed using commercial Bruker NMR spectrometers. Echoes were always read out at $t = t_p$. Short evolution times t_p should ensure that mainly quadrupolar order is created after the first 45° pulse [3,4]. In that case S_2 is directly proportional to a single-particle correlation function. The SAE decay in Fig. 1 clearly proceeds in two steps. The first one, which reflects the hopping correlation function and which can be described here by a slightly stretched exponential $S_0 \exp[-(t_m/\tau)^\gamma]$ with $\gamma = 0.8$, directly yields the jump rate τ^{-1}. The second decay step arises simply from spin-lattice relaxation processes and follows a single exponential. As expected for a jump rate, τ^{-1} is frequency independent ($32 \leq \omega_0/2\pi \leq 155$ MHz). Jump rates from SAE NMR ranging from the sub-Hz to the kHz regime are shown in Fig. 2 vs reciprocal temperature $1/T$. Arrhenius behavior $\tau^{-1}(1/T) = \tau_0^{-1} \exp(-E_A/k_BT)$ with an activation energy $E_A = 0.37(1)$ eV and a preexponential factor $\tau_0^{-1} = 1.0(5) \times 10^{12}$ s^{-1} is found. k_B is Boltzmann's constant. Below 220 K (rigid-lattice regime) τ^{-1} can be well separated from the influence of spin-lattice relaxation. The upper and lower limit of detectable jump rates is given by T_1^{-1} and T_2^{-1}, i.e., $T_1^{-1} < \tau^{-1} < T_2^{-1}$.

Faster Li jump rates can be estimated by T_2^{-1} and probed by T_1^{-1} measurements, respectively. The spectrometer setup is the same as described in Ref. [17]. The investigation of $T_2^{-1}(1/T)$ can be used to estimate τ^{-1} when ionic diffusion is fast enough to affect spin-spin relaxation. However, Li jump rates below 10^4 s^{-1} are hardly or not detectable via T_2 measurements. From SAE NMR $\tau^{-1} \approx 10^4$ s^{-1} at 240 K is predicted after extrapolating the Arrhenius fit in Fig. 2 to higher T. In fact, at about 240 K the rates T_2^{-1} start to decrease, i.e., $\tau^{-1} \approx 1/T_{20} = 1/100\ \mu$s, in perfect agreement with the results from SAE NMR. T_{20} is the rigid-lattice value of T_2. Much higher Li jump rates can be determined from the frequency dependent positions of the diffusion induced relaxation peaks $T_{1\mathrm{diff}}^{-1}(1/T)$.

In general, the peak shows up at $1/T_{\max}$, when the ionic jump rate τ^{-1} reaches ω_0, i.e., in the case of 2D diffusion, when $\tau^{-1}(1/T_{\max}) \cong \frac{1}{2}\omega_0$ [18]. Thus, recording $T_{1\mathrm{diff}}^{-1}(1/T)$ for different values of $\omega_0/2\pi$ gives direct

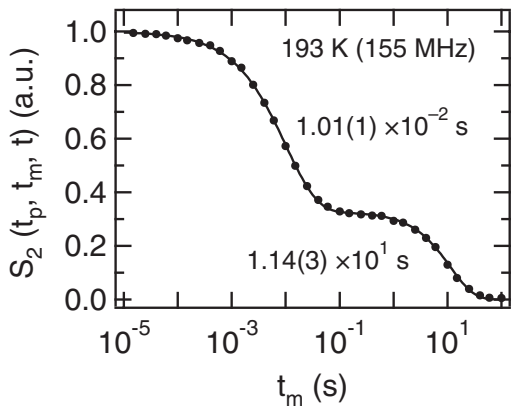

FIG. 1. Semilog plot of normalized ^{7}Li SAE amplitudes of $Li_{0.7}TiS_2$ vs t_m ($t = t_p = 15\ \mu$s) at 193 K. The first decay step directly yields the Li residence time $\tau = 1.01(1) \times 10^{-2}$ s, whereas the second decay step simply reflects T_1 relaxation, $T_1 \approx 1.1 \times 10^1$ s. The solid line represents a fit according to the sum of a stretched (τ) and a single exponential (T_1).

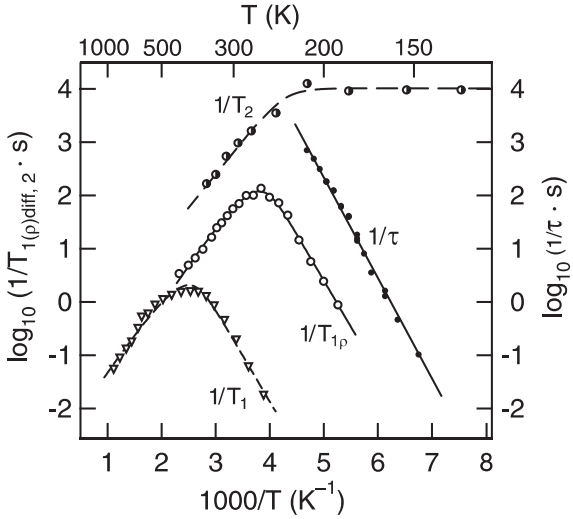

FIG. 2. Li jumps rates τ^{-1} (●) vs $1/T$ directly measured by SAE NMR in comparison with the $T_{1\mathrm{diff}}^{-1}$ (▽ 9.97 MHz) and $T_{1\varrho\mathrm{diff}}^{-1}$ (○ 5.2 kHz) data. The dashed and solid lines are fits according to the Richards expression (see text). Constant T_2^{-1} rates (◑) below 220 K mark the rigid-lattice regime.

access to different pairs of variates $\tau^{-1}(1/T_{\max})$. This allows the measurement of model-independent jump rates τ^{-1}, which can be used to compare with those obtained directly by SAE NMR, but on a much longer time scale. Usually, ω_0 is of the order of some hundreds MHz, so that very fast Li motions are measured. Slower ionic motions, however, can be probed by recording spin-lattice relaxation rates $T_{1\varrho\mathrm{diff}}^{-1}$ in the rotating frame. The position of the corresponding relaxation peak is determined by the locking frequency $\omega_1/2\pi$, which is of the order of several kHz. The first example of this technique was given by Ailion *et al.* [8]. NMR relaxation rate peaks of $Li_{0.7}TiS_2$ are shown together with the SAE NMR data in Fig. 2. Li activation energies E_A^{low} obtained from the slope of the low-T flank of the $T_{1\mathrm{diff}}^{-1}$ and $T_{1\varrho\mathrm{diff}}^{-1}$ peaks are similar. Values slightly smaller than 0.4 eV are obtained, agreeing with $E_A = 0.37(1)$ eV measured by SAE NMR. In Fig. 3 jump rates τ^{-1} vs T^{-1} obtained from SAE NMR, from T_2^{-1}, $T_{1\varrho\mathrm{diff}}^{-1}$ as well as from the $T_{1\mathrm{diff}}^{-1}$ measurements are shown. Taken together, Li jump rates from 10^{-1} to 10^9 s^{-1} were measured directly. These values obey the Arrhenius relation $\tau^{-1} = 6.3(1) \times 10^{12}\ s^{-1} \exp(-0.41(1)\ \mathrm{eV}/k_B T)$, where the preexponential factor is in the typical range of phonon frequencies. It should be noted that the so obtained jump rates precisely fit together without any adjustment. This shows on the one hand that, remarkably, one and the same diffusion process is effective over the whole dynamic range in this 2D model compound. Apparently, this is a two-site jump process between 1b and 2d positions (see above), which is energetically the most favorable pathway for Li migration in layered $Li_{0.7}TiS_2$ as well as in isostructured Li_xTiSe_2 [19]. On the other hand, we come to the nontrivial conclusion that different methods probing *a priori* different correlation functions are able to yield identical diffusion parameters if the underlying diffusion process is the same.

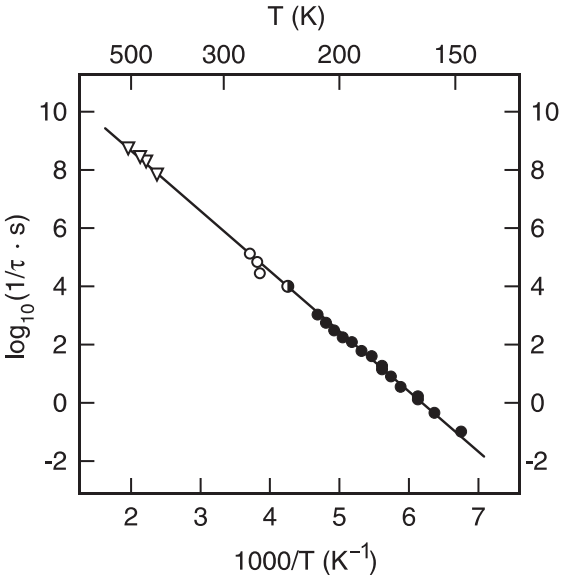

FIG. 3. Li jump rates for $Li_{0.7}TiS_2$ vs $1/T$. Model-independent jump rates were obtained from the diffusion induced NMR relaxation maxima at different resonance (▽: 9.97, 19.2, 27.9, and 77.7 MHz) and locking frequencies (○: 2.1, 5.2, and 10 kHz) and directly via ^{7}Li SAE NMR correlation functions (●: 155 MHz and $t_p = 15$ μs). Furthermore, at 240 K the jump rate τ^{-1} (◑) can be estimated from T_2^{-1} ($\omega_0/2\pi = 155$ MHz). The solid line corresponds to $\tau^{-1} = 6.3(1) \times 10^{12}\ s^{-1} \times \exp(-0.41(1)\ \mathrm{eV}/k_B T)$.

In addition to the investigation of Li jump rates, NMR relaxation also serves as a tool for studying the dimensionality of diffusion processes, even in a polycrystalline material [1]. Besides the temperature, in particular, the frequency dependence of $T_{1\mathrm{diff}}^{-1}$ and $T_{1\varrho\mathrm{diff}}^{-1}$ has to be investigated for this purpose. The 2D nature of Li diffusion in $Li_{0.7}TiS_2$ was unambiguously confirmed in our group before by the logarithmic frequency dependence of $T_{1\mathrm{diff}}^{-1}$ and $T_{1\varrho\mathrm{diff}}^{-1}$ on the high-T flank ($\omega_0\tau \ll 1$ and $\omega_1\tau \ll 1$, respectively) [20]. On the low-T side ($\omega_0\tau \gg 1$), however, as expected when correlation effects have only a small influence on $T_{1\mathrm{diff}}^{-1}$, a nearly quadratic frequency dependence $T_{1\mathrm{diff}}^{-1} \propto \omega_0^{-\beta}$ is observed here (generally $1 < \beta \leq 2$; see below). Furthermore, as can be seen in Fig. 2 the $T_{1\varrho\mathrm{diff}}^{-1}(1/T)$ peak exhibits a reduced slope on the high-T side [21] compared to that on the low-T side, as expected for low-dimensional diffusion [1,22]. Besides the T_1^{-1} and $T_{1\varrho}^{-1}$ measurements, the T_2^{-1} data also confirm the 2D nature of Li diffusion. Extrapolating the T_2^{-1} values to the range $T > 500$ K (cf. Figure 2), we have $T_1/T_2 \gg 1$. This occurs and is expected because of the anomalously large secular (independent of ω_0) contribution to T_2 for low dimensions (1D, 2D); cf. Ref. [22]. In order to describe the temperature and frequency dependence of the spin-lattice relaxation rates for a 2D system, the two limiting cases for low [$\omega\tau \gg 1$: $T_1^{-1}(\omega, \tau) \propto \omega^{-\beta}\tau^{-1}$] and high temperatures [$\omega\tau \ll 1$: $T_1^{-1}(\omega, \tau) \propto \tau \ln(1/\omega\tau)$] were combined by Richards [18] in the empirical expression for the spectral density $J_{2D}(\omega, \tau) \propto T_1^{-1}(\omega, \tau)$ with $J_{2D}(\omega, \tau) \propto \tau \ln(1 + 1/(\omega\tau)^{\beta})$. Here, ω and T_1^{-1} are used for both, ω_0 and ω_1, and $T_{1\varrho\mathrm{diff}}^{-1}$ and $T_{1\mathrm{diff}}^{-1}$, respectively. Plotting $J_{2D}(\omega, \tau) \propto T_1^{-1}(\omega, \tau)$ vs $1/T$ with $\beta = 2$ and for fixed ω leads to asymmetric peaks with a reduced slope of the high-T flank resulting in $E_A^{\mathrm{high}} \approx 0.75 \times E_A^{\mathrm{low}}$, where E_A^{high} and E_A^{low} are the activation energies of the high-T and low-T flank, respectively. Fits according to the Richards expression fully agree with the experimental data and are shown in Fig. 2 exemplarily for $\omega_1/2\pi = 5.2$ kHz and $\omega_0/2\pi = 9.97$ MHz, respectively. β turned out to range between 1.9 (9.97 MHz) and 2.0 (5.2 kHz), which indicates an only marginal influence of correlation effects in agreement with the independently studied (quadratic) frequency dependence of $T_{1\mathrm{diff}}^{-1}$ for $\omega_0\tau \gg 1$, mentioned above. Such effects would result in $1 < \beta < 2$ (cf. Refs. [23–25]), and thus in an apparent activation energy smaller than $E_A = E_A^{\mathrm{low}}$. The parameters, E_A and

TABLE I. Comparison of E_A and τ_0^{-1} for Li diffusion in $Li_{0.7}TiS_2$ obtained from the different NMR methods.

NMR method	E_A (eV)		τ_0^{-1} (s^{-1})
SAE[a]	0.37(1)		$1(1) \times 10^{12}$
T_2[b]	0.36(2)		...
	low-T flank	2D Richards-fit[e]	
$T_{1\varrho}$ (5.2 kHz)	0.37(1)[c]	0.35(1)	$3(1) \times 10^{11}$
T_1 (9.97 MHz)	0.37(2)[d]	0.34(2)	$2(1) \times 10^{12}$

[a] $140 < T < 220$ K, rigid-lattice regime.
[b] $250 < T < 360$ K.
[c] $190 < T < 240$ K, low-T flank of the $T_{1\varrho\mathrm{diff}}^{-1}(1/T)$ peak.
[d] $260 < T < 340$ K, low-T flank of the $T_{1\mathrm{diff}}^{-1}(1/T)$ peak.
[e] Cf. Figure 2 for T ranges; β was restricted to ≤ 2.

τ_0^{-1}, used for fitting the Richards expression to the $T_{1\mathrm{diff}}^{-1}$ and $T_{1\varrho\mathrm{diff}}^{-1}$ data, range between $0.34\ \mathrm{eV} \leq E_A \leq 0.38\ \mathrm{eV}$ and $2 \times 10^{11}\ \mathrm{s}^{-1} \leq \tau_0^{-1} \leq 2 \times 10^{12}\ \mathrm{s}^{-1}$, respectively. Furthermore, with τ_0^{-1} and $\langle \Delta\omega^2 \rangle$ being the dipolar second moment of ^{7}Li in $Li_{0.7}TiS_2$, $E_A = 0.36(2)$ can be estimated from the slope $d(\ln T_2^{-1})/d(1/(k_B T))$ of the spin-spin relaxation rates for $T > 240$ K taking into account the dimensionality $d = 2$ of the diffusion process [22]. In Table I the main experimental results from the four NMR methods are listed for comparison. The excellent agreement of the results shows up in identical values for E_A and τ_0^{-1}, revealing the presence of one single diffusion process in layer-structured $Li_{0.7}TiS_2$. E_A is equal to those values measured by electrochemical methods; see, e.g., Ref. [26]. Measurements of the ionic electrical conductivity of the sample investigated here are in progress in our laboratory. Additionally, SAE NMR and conductivity experiments on the other polymorph of $Li_{0.7}TiS_2$, viz cubic one which is a 3D ionic conductor, are planned to compare with those obtained for the 2D model system studied in this work.

In summary, ^{7}Li SAE NMR measurements as well as T_1, $T_{1\varrho}$, and T_2 experiments were employed to investigate Li diffusion in polycrystalline $Li_{0.7}TiS_2$ serving here as a model substance for two-dimensional cation diffusion. Combining these four NMR methods, Li diffusion was probed on quite different (length and) time scales (sub-Hz to GHz range). The results are entirely consistent with each other and give evidence for one single diffusion process over a dynamic range of about ten decades and with an activation energy of about 0.4 eV. Jump rates measured directly by ^{7}Li SAE NMR at very low temperatures are fully consistent with those obtained from the maxima of the diffusion induced ^{7}Li NMR relaxation peaks, i.e., directly without involving a specific model. Beyond doubt the temperature and frequency dependent NMR relaxation measurements confirm the simple expression introduced by Richards for 2D diffusion. In conclusion, the study of 2D diffusion in lithium titanium disulfide by NMR yields a highly consistent picture, being suitable to become a textbook example.

Financial support by the Deutsche Forschungsgemeinschaft (DFG) is gratefully acknowledged.

*Electronic address: wilkening@pci.uni-hannover.de
†Electronic address: heitjans@pci.uni-hannover.de

[1] P. Heitjans, A. Schirmer, and S. Indris, in *Diffusion in Condensed Matter-Methods, Materials, Models*, edited by P. Heitjans and J. Kärger (Springer, Berlin, 2005).
[2] H. W. Spiess, J. Chem. Phys. **72**, 6755 (1980).
[3] X.-P. Tang, R. Busch, W. L. Johnson, and Y. Wu, Phys. Rev. Lett. **81**, 5358 (1998); X.-P. Tang, U. Geyer, R. Busch, W. L. Johnson, and Y. Wu, Nature (London) **402**, 160 (1999).
[4] F. Qi, T. Jörg, and R. Böhmer, Solid State Nucl. Magn. Reson. **22**, 484 (2002).
[5] Z. Xu and J. F. Stebbins, Science **270**, 1332 (1995).
[6] V. W. J. Verhoeven, I. M. de Schepper, G. Nachtegaal, A. P. M. Kentgens, E. M. Kelder, J. Schoonman, and F. M. Mulder, Phys. Rev. Lett. **86**, 4314 (2001).
[7] L. S. Cahill, R. P. Chapman, J. F. Britten, and G. R. Goward, J. Phys. Chem. B **110**, 7171 (2006).
[8] D. C. Ailion and C. P. Slichter, Phys. Rev. **137**, A235 (1965).
[9] R. Messer and F. Noack, Applied Physics (Berlin) **6**, 79 (1975).
[10] P. Heitjans, A. Körblein, H. Ackermann, D. Dubbers, F. Fujara, and H.-J. Stöckmann, J. Phys. F **15**, 41 (1985).
[11] M. S. Whittingham, Prog. Solid State Chem. **12**, 41 (1978).
[12] J. R. Dahn, W. R. McKinnon, R. R. Haering, W. J. L. Buyers, and B. M. Powell, Can. J. Phys. **58**, 207 (1980).
[13] F. Mendizábal, R. Contreras, and A. Aizman, J. Phys. Condens. Matter **9**, 3011 (1997).
[14] T. Bredow, P. Heitjans, and M. Wilkening, Phys. Rev. B **70**, 115111 (2004).
[15] J. Jeener and P. Broekaert, Phys. Rev. **157**, 232 (1967).
[16] M. Wilkening, Ph.D. thesis, University of Hannover, 2005.
[17] W. Franke and P. Heitjans, Ber. Bunsen-Ges. Phys. Chem. **96**, 1674 (1992).
[18] P. M. Richards, Solid State Commun. **25**, 1019 (1978).
[19] C. Ramírez, R. Adelung, R. Kunz, L. Kipp, and W. Schattke, Phys. Rev. B **71**, 035426 (2005).
[20] W. Küchler, P. Heitjans, A. Payer, and R. Schöllhorn, Solid State Ionics **70/71**, 434 (1994).
[21] A significant contribution of T_1^{-1} to the high-T flank of the $T_{1\varrho}^{-1}$ peaks can be excluded as the $T_{1\varrho}^{-1}$ data were recorded at $\omega_0/2\pi = 77.7$ MHz, i.e., $T_1^{-1} \ll T_{1\varrho}^{-1}$ below $T = 400$ K.
[22] P. M. Richards, in *Topics in Current Physics*, edited by M. B. Salamon (Springer, Berlin, 1979), Vol. 15.
[23] M. Meyer, P. Maass, and A. Bunde, Phys. Rev. Lett. **71**, 573 (1993).
[24] K. L. Ngai, Comments Solid State Phys. **9**, 141 (1980).
[25] K. Funke, Prog. Solid State Chem. **22**, 111 (1993).
[26] K. Kanehori, F. Kirino, T. Kudo, and K. Miyauchi, J. Electrochem. Soc. **138**, 2216 (1991).